

# Finite indentation of highly curved elastic shells

S.P.Pearce<sup>1,2</sup>, J.R.King<sup>3</sup>, N.M.Everitt<sup>4</sup>, and M.J.Holdsworth<sup>5</sup>

<sup>1</sup>*School of Mathematics, University of Manchester, UK*

<sup>2</sup>*Faculty of Biology, Medicine and Health, University of Manchester, UK*

<sup>3</sup>*School of Mathematical Sciences, University of Nottingham, UK*

<sup>4</sup>*Bioengineering Research Group, Faculty of Engineering, University of Nottingham, UK*

<sup>5</sup>*Division of Plant and Crop Science, School of Biosciences, University of Nottingham, UK*

December 6, 2016

## Abstract

Experimentally measuring the elastic properties of a thin-walled curved flexible biological surface is difficult. One technique which may be used is the indentation of a thin sheet of material by a rigid indenter, whilst measuring the force or displacement applied to the indenter. This gives immediate information on the fracture strength of the material (from the force required to puncture), but it is also possible to determine the elastic properties by comparing the resulting force-displacement curves with a mathematical model. Mathematical studies of this process commonly assume that the elastic surface is initially flat, which is often not the case for biological membranes. As such, we previously outlined a theory for the indentation of curved isotropic, incompressible, hyperelastic membranes (with no bending stiffness), which breaks down for highly curved surfaces, as the entire membrane becomes wrinkled. Here we treat the surface as an elastic shell by including bending stiffness, ensuring that energy is required to change the shape of the shell even without stretching. The theory presented here enables curved surfaces to be considered in particular, allowing the estimation of shape- and size-independent elastic properties from indentation experiments, and is particularly relevant for biological membranes.

## 1 Background

The experimental characterisation of the elastic properties of a curved flexible shell is of interest within both biological and engineering contexts. Throughout plant and animal biology, surfaces often grow with

a three-dimensional structure, leading to complex curved shapes [1]. Such structures are not amenable to the majority of engineering techniques to determine elastic properties, such as vibration or tensile tests, since test-piece shapes must be controlled. Indentation tests, in which a rigid indenter is pushed into the specimen, have been performed and modelled for flat surfaces [2; 3; 4; 5; 6; 7; 8; 9], but little attention has been paid to curved surfaces, with Deris and Nadler [10] who consider the indentation of a fluid filled spherical membrane being a recent exception. When curved surfaces are used, the context is often that of atomic force microscopy (AFM) or nano-indentation, where the indentation depth and needle size are much smaller than the surface itself, for example in Vella et al. [11, 12].

There are also similarities between this indentation problem and the shaft-loaded blister test [13; 14; 15], where the delamination of a flat elastic surface from a rigid substrate is measured by indentation. The results here may therefore also be useful for extending the blister-test analysis to non-flat surfaces.

In Pearce et al. [16] we considered the indentation of a curved elastic membrane by a large rigid indenter, finding that such curved elastic membranes are prone to wrinkling, forming straight tension lines when indented, such as those which may be seen when pushing into a plastic film (such as a shrink-wrap) that is initially curved. Such wrinkling occurs when compressive (negative) stress resultants occur in the membrane, causing a local buckling and the occurrence of creases [17; 18] orthogonal to the compressive stress resultant. In Pearce et al. [16], the tension-field theory was utilised in order to predict the average shape after this instability has occurred. This theory works well for moderately curved membranes, but for more curved membranes this theory gives deformations which are non-local, even for small indentation. This is due to the lack of bending stiffness in the membrane equations, meaning no energy is used to bend the membrane without stretching. In addition, when the initial shape of the membrane is sufficiently curved, no solution may be found for small indentations of the equations as given in Pearce et al. [16], as both of the principal stretches become less than one, and the membrane becomes entirely slack.

In order to address these issues, we use here a shell theory instead of a membrane theory, regularising the singular problem by introducing higher order terms involving resistance to bending into the governing equations. In doing so we are able to find solutions for highly curved shells, and solutions for small indentation distances generate only localised deformations of the shell.

Our particular motivation for considering this indentation problem remains the puncture-force experiments performed on biological materials such as seeds of the Brassicaceae species *Lepidium sativum* (common cress) [19], in which the endosperm of the seed is punctured with a metal needle, the position and force of which are measured. In *Lepidium*, the endosperm may be approximated by a prolate spheroid with major axis three times larger than the two minor axes, hence our interest in highly curved initial surfaces. The application of this theory to determine the elastic properties in these experiments will be presented elsewhere.

## 2 Mathematical Formulation

### 2.1 Governing Equations

We shall use the theory of nonlinear elasticity to model how a thin shell deforms under the action of the indenter, with the prescribed midsurface of the undeformed (or reference) shell defined parametrically by

$$\mathbf{X} = R(S)\mathbf{e}_R(\Theta) + Z(S)\mathbf{e}_Z, \quad 0 \leq S \leq L, \quad 0 \leq \Theta \leq 2\pi, \quad (2.1)$$

where  $S$  shall be the independent variable throughout this work and we are using cylindrical coordinates. If the shell is initially spheroidal, we have  $R(S) = \sin S$ ,  $Z(S) = \gamma \cos S$ , where  $a$  is a parameter that controls the eccentricity and its sign compared to the indenter controls the direction of indentation. In this case,  $S$  is therefore the angle made with the axis of symmetry. If the shell is initially flat then  $R(S) = S$ ,  $Z(S) = 0$ , and here  $S \equiv R$ . While Figure 1 shows an indentation from the concave side of the shell ( $\gamma < 0$ ), this theory is also valid for indentation into the convex side.

The origin of our coordinates lies directly under the indenter, at which point we require the smoothness conditions,  $R(0) = 0$ ,  $Z'(0) = 0$ . The system will be invariant to rigid body movement in the  $Z$ -direction, so for convenience we choose  $Z$  such that  $Z(L) = 0$ . We consider deformations which map the reference

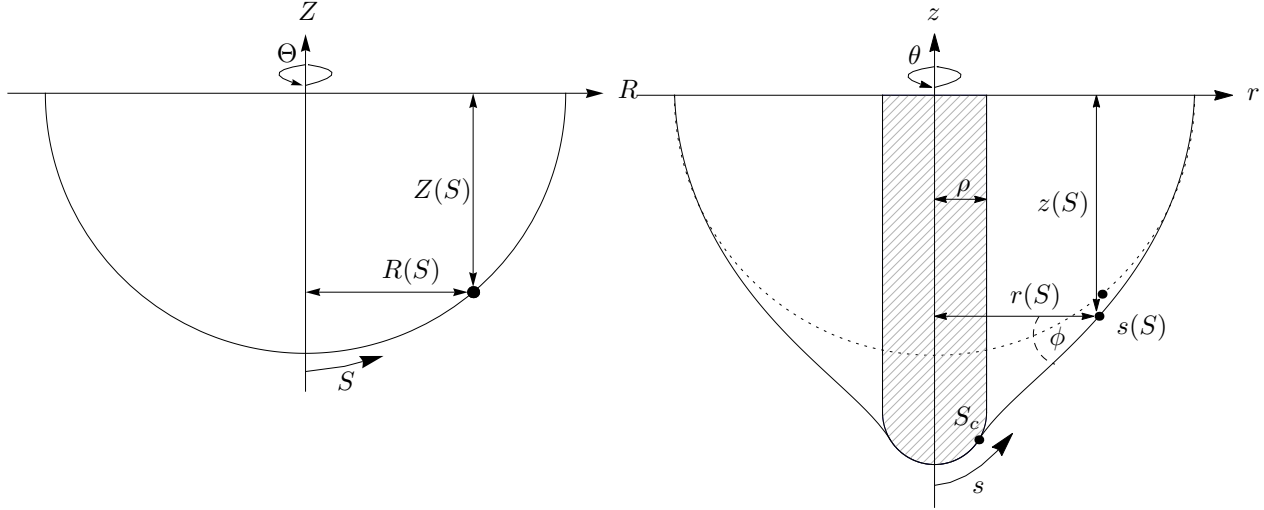


Figure 1: Sketch of the two coordinate systems, the reference and deformed configurations.

configuration  $\mathbf{X}$  onto the deformed configuration  $\mathbf{x}$ , the midsurface of which is given by

$$\mathbf{x} = r(S)\mathbf{e}_R(\theta) + z(S)\mathbf{e}_Z, \quad 0 \leq S \leq L, \quad 0 \leq \theta \leq 2\pi, \quad (2.2)$$

where we keep the same coordinate basis for simplicity. We assume that the initial configuration is axisymmetric and that the deformed configuration remains axisymmetric, which implies that  $\Theta = \theta$ , and we impose the same smoothness conditions at the origin as in the reference configuration,  $r(0) = 0, z'(0) = 0$ . We solve the quasi-steady problem here, on the physical grounds that the indentation is sufficiently slow that inertial effects may be ignored. The principal stretch ratios may be defined in the tangential, azimuthal, and normal directions in the form

$$\lambda_s = \frac{ds}{dS} = \frac{\sqrt{\left(\frac{dr}{dS}\right)^2 + \left(\frac{dz}{dS}\right)^2}}{\sqrt{\left(\frac{dR}{dS}\right)^2 + \left(\frac{dZ}{dS}\right)^2}} \equiv \frac{\psi}{\Psi}, \quad \lambda_\theta = \frac{r}{R}, \quad \lambda_n = \frac{h}{H}, \quad (2.3)$$

where  $h$  and  $H$  are the deformed and undeformed thicknesses respectively,  $s$  is the position in the deformed configuration, as in [16] and  $\psi, \Psi$  are defined for convenience as the radicals in (2.3)<sub>1</sub>. The principal curvatures,  $\kappa_s, \kappa_\theta$ , are defined by

$$\kappa_s = \frac{1}{r'} \left( \frac{z'}{\psi} \right)' = -\frac{1}{z'} \left( \frac{r'}{\psi} \right)', \quad \kappa_\theta = \frac{z'}{r\psi}. \quad (2.4)$$

Curvatures in the reference configuration may be defined in the equivalent way but with respect to the  $R$  and  $Z$  coordinates, i.e.

$$\kappa_s^R = \frac{1}{R'} \left( \frac{Z'}{\Psi} \right)' = -\frac{1}{Z'} \left( \frac{R'}{\Psi} \right)', \quad \kappa_\theta^R = \frac{Z'}{R\Psi}. \quad (2.5)$$

We also note that the curvatures are related by Codazzi's equation,

$$(r\kappa_\theta)' = r'\kappa_s. \quad (2.6)$$

and the tangent,  $\mathbf{e}_s = (r'\mathbf{e}_r + z'\mathbf{e}_z)/\psi$ , and normal,  $\mathbf{n} = (z'\mathbf{e}_r - r'\mathbf{e}_z)/\psi$ , vectors are related by the Frenet-Serret equations,

$$\mathbf{e}_s' = -\kappa_s\psi\mathbf{n}, \quad \mathbf{n}' = \kappa_s\psi\mathbf{e}_s, \quad (2.7)$$

both of these equations also hold for the reference configuration with appropriate substitutions. As described in Pearce et al. [16], the equilibrium equations for a membrane in the tangential and normal directions are respectively given by

$$(r\tau_s)' - r'\tau_\theta = 0, \quad (2.8a)$$

$$\kappa_s\tau_s + \kappa_\theta\tau_\theta = P, \quad (2.8b)$$

where  $P(S)$  represents the pressure difference across the membrane in the normal direction and  $\tau_s, \tau_\theta$  are the principal stress resultants per unit length in the deformed shell (after integrating over the thickness). This system (2.8) may be written as a third order system of ODEs in  $\lambda_s, \lambda_\theta, \kappa_\theta$ , or equivalently as a third order system in  $r, r', z'$ , as  $z$  does not appear explicitly.

When a thin-walled elastic shell is considered instead, by including bending moments, the governing equations which are commonly used are a generalisation of those in (2.8), in our notation being written as [20; 21; 22; 23]

$$(r\tau_s)' - r'\tau_\theta + \kappa_s r Q \psi = 0, \quad (2.9a)$$

$$\kappa_s \tau_s + \kappa_\theta \tau_\theta - \frac{1}{r\psi} (rQ)' = P, \quad (2.9b)$$

$$(rM_s)' - r'M_\theta - rQ\psi = 0, \quad (2.9c)$$

where  $M_s, M_\theta$  are the bending moments in the corresponding directions and  $Q$  is the transverse stress resultant (shear stress). Equations (2.9) have been well studied by a number of authors and generally assuming that the reference configuration is given by either a flat plate or spherical shell, and hence  $\sqrt{R'^2 + Z'^2} = 1$ . They are also often written in Eulerian coordinates, with derivatives given as  $\frac{d}{ds} = \psi^{-1} \frac{d}{dS}$ , particularly when stretching is entirely neglected in favour of bending. In (2.9), the first two equations are the force balances in the tangential and normal directions, and the third equation is the balance of bending forces. The membrane limit (2.8) is therefore given by (2.9) with  $M_s, M_\theta$  both tending to zero.

We may integrate (2.9), with the help of (2.6), to give the resultant force in the  $Z$ -direction as (assuming that the pressure  $P$  is constant)

$$r^2 \kappa_\theta \tau_s - \frac{rr'Q}{\psi} = \int_0^S P r r' dS + \frac{F(S)}{2\pi}, \quad (2.10)$$

where we have defined the net axial force acting on the shell between the origin and  $S$  as  $F(S)$ , generated by the indenter. We will assume here that the pressure difference comes solely from the indenter, although the indentation of a pressurised membrane (such as a balloon or vesicle) may be incorporated into the framework presented here. As we are treating the indentation as a quasi-static process,  $F$  is a function solely of  $S$ , with the experimentally measured force therefore being  $F(L)$ . If the term involving the pressure in (2.10) is explicitly integrable, such as when  $P$  is constant, we may use this equation to reduce the order of the system by one if we wish.

## 2.2 Stress Resultants

Following the procedure in Steigmann and Ogden [24], Sanders and Lyell [25] or Yeung [26], the virtual work done by the shell may be written as:

$$\dot{E} = \iint dA \left[ (T_s + M_s \kappa_s) \frac{\dot{\lambda}_s}{\lambda_s} + (T_\theta + M_\theta \kappa_\theta) \frac{\dot{\lambda}_\theta}{\lambda_\theta} + M_s \dot{\kappa}_s + M_\theta \dot{\kappa}_\theta \right], \quad (2.11)$$

where  $T_s$  and  $T_\theta$  are planar stress resultants and dots indicate the variation of a quantity. This expression may be derived from three-dimensional theory by integration through the thickness [25; 26], assuming the Kirchhoff hypotheses.

We can thus see that the moment resultants are conjugate to the virtual changes in curvature, but the terms conjugate to the virtual changes in the stretches are "generalised tensions" [26], which take the form of tension plus curvature times bending moment. It is these generalised tension stress resultants that feature in (2.9), and they therefore should be of this generalised form, including the  $M\kappa$  terms, and so we will define

$$\tau_s = T_s + \nu M_s \kappa_s, \quad \tau_\theta = T_\theta + \nu M_\theta \kappa_\theta, \quad (2.12)$$

where the parameter  $\nu \in \{0, 1\}$  is zero for the commonly used approximation and one for the full expansion as required by (2.11). These additional terms come from the fact that the element under consideration is actually curved rather than flat, and they tend to be neglected in the derivations which lead to (2.9). In this case we find that when the shell is highly curved, these terms become significant and cannot be ignored; an explanation in Cartesian coordinates is found in Article 328 of Love [27]. These additional terms appear naturally in the theories of Steigmann and Ogden [24], as well as others [28; 29; 30; 25] which derive the governing equations from a variational principle as opposed to a force balance. The necessity of these terms in the buckling of liposomes is discussed in Pamplona et al. [22]. Similar terms are used in Blyth and Pozrikidis [31] and Evans and Yeung [32], but with the opposing curvatures in the additional terms, e.g.  $\tau_s = T_s + M_s \kappa_\theta$ , this may have come from the presence of these opposing curvatures in the definition of the integrals in the three-dimensional theory.

### 2.3 Constitutive Equations

It remains to specify the constitutive equations relating the stresses and bending moments to the stretches and curvatures. For a membrane we would now simply suppose the existence of a strain-energy function  $W(\lambda_s, \lambda_\theta, \lambda_n)$ , where we assume that the material is incompressible and therefore set  $\lambda_n = \lambda_s^{-1} \lambda_\theta^{-1}$  [33]. The principal stress resultants per unit length in the deformed shell are then defined from  $T_\alpha = h \sigma_\alpha$ ,  $\alpha \in \{s, \theta\}$ , where  $\sigma_\alpha = \lambda_\alpha \frac{\partial W}{\partial \lambda_\alpha}$  is the usual principal Cauchy stress in incompressible three-dimensional elasticity, leading to

$$T_s = \frac{H \lambda_s}{\lambda_s \lambda_\theta} \frac{\partial W}{\partial \lambda_s}, \quad T_\theta = \frac{H \lambda_\theta}{\lambda_s \lambda_\theta} \frac{\partial W}{\partial \lambda_\theta}. \quad (2.13)$$

For further details see Naghdi and Tang [34], Haughton [35] and Pearce et al. [16]. While the theory presented here is appropriate for any isotropic incompressible strain-energy function, but we will show examples with the Mooney-Rivlin material model,

$$W = \frac{\mu}{2} [(1 - \alpha) (\lambda_s^2 + \lambda_\theta^2 + \lambda_s^{-2} \lambda_\theta^{-2} - 3) + \alpha (\lambda_s^{-2} + \lambda_\theta^{-2} + \lambda_s^2 \lambda_\theta^2 - 3)],$$

where  $\mu$  is the shear modulus and  $\alpha$  controls the deviation from the neo-Hookean response (which is given by  $\alpha = 0$ ).

However, as we want to include the dependence of the energy on the effect of bending, it is necessary also to give a constitutive equation for the bending moments. Appropriate forms for these dependencies are not clear in the literature, various assumptions are often being made without any clear mathematical justification or only applying in specific cases, such as area conserving deformations. Here we shall follow the derivation of Steigmann and Ogden [24] for the deformation of a two-dimensional elastic surface, where the higher order bending effects are dependent on the strain gradient  $\nabla \mathbf{F}$ , where  $\mathbf{F}$  is the surface deformation gradient, thereby incorporating only the elastic resistance to flexure in addition to the standard strain resistance. This leads to an energy per unit area given by  $U(\mathbf{C}, \mathbf{\Delta}; \mathbf{X})$ , where  $\mathbf{C} = \mathbf{F}^T \mathbf{F}$  is the right Cauchy-Green tensor and  $\mathbf{\Delta} = \boldsymbol{\kappa} - \boldsymbol{\kappa}^R$  is the relative curvature strain tensor (see the Appendix and Steigmann and Ogden [24] for details). The invariants of the curvature strain tensor are given by

$$I_3 = \text{tr} \mathbf{\Delta} = \lambda_s^2 \kappa_s + \lambda_\theta^2 \kappa_\theta - \kappa_s^R - \kappa_\theta^R, \quad (2.14)$$

$$I_4 = \det \mathbf{\Delta} = (\lambda_s^2 \kappa_s - \kappa_s^R)(\lambda_\theta^2 \kappa_\theta - \kappa_\theta^R), \quad (2.15)$$

where for simplicity we have neglected any dependence on the three further invariants including the coupling between  $\mathbf{C}$  and  $\mathbf{\Delta}$  for simplicity. We explicitly note that the invariants of  $\mathbf{\Delta}$  involve both the stretches and the curvatures, which means that the bending moments should be based on these kind of mixed terms, not just relative curvature changes. As the shell is isotropic, the energy must be invariant under the rotation of the coordinate system and hence an even function of  $I_3$ , so the simplest appropriate form for the energy  $U$  is

$$U = W(\lambda_s, \lambda_\theta) + \frac{B}{2} I_3^2, \quad (2.16)$$

where  $B$  is a bending modulus and we choose not to involve the Gaussian curvature  $I_4$ . The bending moments are thus given by

$$M_s = h \frac{\partial U}{\partial \kappa_s} = BH \frac{\lambda_s^2}{\lambda_s \lambda_\theta} (\lambda_s^2 \kappa_s + \lambda_\theta^2 \kappa_\theta - \kappa_s^R - \kappa_\theta^R), \quad (2.17a)$$

$$M_\theta = h \frac{\partial U}{\partial \kappa_\theta} = BH \frac{\lambda_\theta^2}{\lambda_s \lambda_\theta} (\lambda_s^2 \kappa_s + \lambda_\theta^2 \kappa_\theta - \kappa_s^R - \kappa_\theta^R). \quad (2.17b)$$

Other constitutive equations for combined bending and stretching have been used within the literature [22; 31; 21] but these do not involve the invariants as presented above, as they are presented as ad-hoc assumptions.

For incompressible linear elasticity, the bending modulus  $B$  is proportional to the shear modulus [20]

$$B = \frac{\mu H^2}{12}. \quad (2.18)$$

### 3 Solution Procedure

When written in terms of  $r$  and  $z$ , (2.9) appears to be a seventh order ODE system (as  $z$  never appears undifferentiated). However, the highest order derivatives appear only in combination, so we may reformulate it as a set of five nonlinear first order ODEs in  $(\lambda_s, \lambda_\theta, \kappa_s, \kappa_\theta, Q)$ , with (2.6) and (2.3)<sub>1</sub> providing two further equations, after which  $z$  may be found by integrating  $z' = r\psi\kappa_\theta$ .

To avoid square roots in the numerical calculations, we introduce  $\phi$ , the angle between the axis of revolution and the normal to the meridian in the deformed configuration (see Figure 1), defined by

$$\frac{dr}{ds} = \frac{r'}{\psi} = \cos \phi, \quad \frac{dz}{ds} = \frac{z'}{\psi} = \sin \phi, \quad \kappa_\theta = \frac{\sin \phi}{r}, \quad \kappa_s = \frac{\phi'}{\psi}. \quad (3.19)$$

The undeformed domain will be split into two regions, based on whether their corresponding material points are in contact with the indenter or not, with the boundary circle being given by  $S = S_c$ . This contact circle is unknown *a priori*, and must be determined as part of the solution, and so we therefore need to give six boundary conditions to close the fifth-order system.

#### 3.1 Indenter Region

We assume the shell is indented by a rigid indenter consisting of a cylinder with radius  $\rho$  connected to a tip which is described parametrically in terms of an angle  $\omega$  by  $r = \rho A(\omega)$ ,  $z = \rho B(\omega)$ , for some specified shape given by  $(A, B)$ . We also impose the axisymmetry requirements  $A(0) = 0$ ,  $B'(0) = 0$  at the axis, and hence only consider smooth indenter tips. Indentation by an isolated sphere or other axisymmetric object under gravity could also be accommodated in the same framework. In the region of the shell in contact with the indenter, we assume that the shell conforms precisely to the shape of the indenter, prescribing both  $r$  and  $z$  there, although the stretch in this contact region is still unknown; we assume there is no slip between the indenter and the shell. We therefore let

$$r(S) = \rho A(\omega(S)), \quad z(S) = -\delta + \rho B(\omega(S)), \quad (3.20)$$

where  $\delta$  is the depth of indentation, to be found as part of the solution, and we treat the angle  $\omega$  in the deformed configuration as a function of  $S$ . Therefore in the contact region,

$$\lambda_s = \rho \frac{\sqrt{A'(\omega(S))^2 + B'(\omega(S))^2}}{\Psi} \frac{d\omega}{dS}, \quad \lambda_\theta = \rho \frac{A(\omega(S))}{R(S)}, \quad (3.21)$$

where we have used  $\omega'(S) > 0$ . We may then evaluate the first equilibrium equation, (2.9a), to find  $\omega(S)$  given appropriate boundary conditions, having solved the third equilibrium equation (2.9c) for  $Q$ . The



second equilibrium equation (2.9b) enables us to calculate the pressure  $P$  exerted by the indenter on the shell after calculating the deformation (and hence the function  $F$ ), but this is supplemental to computing the deformation itself in the contact region. Equation (2.9a) leads to a second-order differential equation for the deformed angle,  $\omega(S)$ , as the principal curvatures become

$$\kappa_s = \frac{A'(\omega)B''(\omega) - B'(\omega)A''(\omega)}{\rho \omega'(S)(A'(\omega)^2 + B'(\omega)^2)^{3/2}}, \quad (3.22)$$

$$\kappa_\theta = \frac{B'(\omega)}{\rho \omega'(S)A(\omega)\sqrt{A'(\omega)^2 + B'(\omega)^2}}, \quad (3.23)$$

and so  $\kappa_s$  involves  $\omega'(S)$ , as does  $\lambda_s$ , but not  $\omega''(S)$  as might have been expected. This means that the governing equation in the indenter region is second order in  $\omega(S)$ , as in the membrane case.

At the pole,  $S = 0$ , there exists a coordinate-induced singularity in the governing equations, as  $r$  and  $R$  are both zero at this point. We therefore begin the integration in the indenter region at a value  $0 < \zeta \ll 1$ , at which we use the expansions

$$\omega(\zeta) = \zeta \omega'(0) + \mathcal{O}(\zeta^3), \quad \omega'(\zeta) = \omega'(0) + \mathcal{O}(\zeta^2), \quad (3.24)$$

which were also necessary in the membrane case. In (3.24) the symmetry restriction that  $\omega$  is an odd function has been used, and  $\omega(0) = 0$  is one of the required boundary conditions. Using the restrictions on  $A$  and  $B$ , we find  $\omega'(0) = \rho^{-1} \lambda_s(0) R'(0) / A'(0)$ , and we can therefore integrate (2.9a) to find  $\omega(S)$  for a given stretch at the pole  $\lambda_0 \equiv \lambda_s(0) = \lambda_\theta(0)$  and a given constitutive equation (section 2.3). So our boundary conditions at the pole of the contact region are:

$$\omega(\zeta) = \zeta \rho^{-1} \lambda_0 R'(0) / A'(0), \quad \omega'(\zeta) = \rho^{-1} \lambda_0 R'(0) / A'(0). \quad (3.25)$$

We integrate from  $S = \zeta$ , using the expansion (3.24) around zero to avoid the coordinate-induced singularity, to  $S = S_{cyl}$  where the shell contacts the cylindrical part of the indenter, for a given  $\lambda_0$ . Cases of extreme indentation where the cylindrical part of the indenter touches the shell may also be calculated, with appropriate changes to (3.20).

This lets us vary the contact position  $S_c$  from which the integration of the free region begins, in order to satisfy the remaining boundary conditions for that value of  $\lambda_0$ . We note that for small indentations for curved shells there may be a compressive stretch around the pole, with  $\lambda_0 < 1$ , unlike the membrane case.

This method assumes that the indenter first comes into contact with the tip of the shell, and will not work if the side of the shell is touched first, here we require the curvature of the indenter to be less than that of the shell,  $\kappa_\theta^R(0) < B''(0) / (\rho A'(0)^2)$ .

## 3.2 Free Region

Outside of the contact region, the equations (2.9) are a system of five first-order differential equations for  $\lambda_s, \lambda_\theta, \kappa_s, \kappa_\theta, Q$ , and thus require five boundary conditions, with  $P$  being zero as there is no applied pressure in this region. In addition, as we do not know the location of the contact circle,  $S_c$ , at which the continuity conditions will be specified, we require a sixth boundary condition to complete the system. At the fixed boundary  $S = L$  we will apply hinged boundary conditions, inspired by our experimental motivation,  $\lambda_\theta = 1, M_s = 0$ , other boundary conditions are possible. We note that we could include a radial pre-stretch prior to the indentation, by allowing  $\lambda_\theta(L) = \lambda_p > 1$ , but this pre-stretch will necessarily change the shape of the shell prior to indentation and induce significant additional complexity when the surface is not initially flat. This may be relevant when a non-zero internal pressure is included or to account for growth in biological contexts.

At the contact circle, we require continuity of the position,  $r$ , normal,  $\mathbf{n}$ , and the resultant force,  $F$ , giving four continuity conditions. When using the approximate expansion ( $\nu = 0$ ), this implies that  $\lambda_s, \lambda_\theta, \kappa_\theta$  and  $Q$  are continuous. The remaining variable, the curvature  $\kappa_s$ , is allowed to have a jump at the interface, as in the membrane case [16], enabling the shell to change curvature between the forced indenter shape and the remaining free section.

However, when using the full definition for the generalised tensions (2.12) with  $\nu = 1$ , the force  $F$  now includes  $\kappa_s$ , and this then requires  $\lambda_s$  to be discontinuous via a jump in  $\psi$ , while keeping  $\phi$  continuous to ensure continuity in the normal. This ensures that both generalised tensions are continuous across the interface, and we therefore have

$$[[\lambda_\theta]] = [[\kappa_\theta]] = [[Q]] = 0 \quad (3.26a)$$

$$[[F]] = [[r \sin \phi \tau_s - r \cos \phi Q]] = 0 \quad (3.26b)$$

$$\lambda_\theta(L) = 1, \quad M_s(L) = 0, \quad (3.26c)$$

where  $[[x]] = x(S_c^+) - x(S_c^-)$  is the jump in the value of  $x$  across the contact line, closing the system with four continuity conditions at  $S = S_c$  and two boundary conditions at  $S = L$ , and implies  $[[\phi]] = 0$ . It is most convenient numerically to solve (3.26b) for  $\lambda_s(S_c^+)$ , for a given  $\kappa_s(S_c^+)$ .

We then vary the value of  $S_c$  and  $\kappa_s$  in order to satisfy the two boundary conditions at  $S = L$  using a shooting method. So, given the initial size and shape of the indenter and shell, as well as constitutive equations for the shell, we can solve the system above for a specified  $\lambda_0$ . We then calculate the force on the indenter,  $F$ , and the depth of indentation of the shell,  $\delta$ , and then vary  $\lambda_0$  to cover the range of forces and displacements, leading to a force-displacement curve.

### 3.3 Non-dimensionalisation

All the previous expressions involve dimensional quantities, which we will now denote with hats in this section. We now wish to non-dimensionalise by choosing the undeformed radius  $\hat{R}_L = \hat{R}(\hat{L})$  as our characteristic length, and we have the choice of either  $\hat{\mu}\hat{R}_L\hat{H}$  or  $\hat{B}$  as our characteristic force. To be consistent with Pearce et al. [16] and in order to keep the membrane limit approachable without rescaling, we choose  $\hat{\mu}\hat{R}_L\hat{H}$ . Therefore we have

$$\begin{aligned}(\hat{S}, \hat{R}, \hat{Z}, \hat{H}, \hat{r}, \hat{z}, \hat{\rho}, \hat{L}) &= \hat{R}_L(S, R, Z, H, r, z, \rho, L) \\(\hat{T}_s, \hat{T}_\theta, \hat{Q}) &= \hat{\mu}\hat{H}(T_s, T_\theta, Q), \hat{P} = \hat{\mu}P \\ \hat{F} &= \hat{\mu}\hat{R}_L\hat{H}F, \quad \hat{W} = \hat{\mu}W, (\hat{M}_s, \hat{M}_\theta) = \hat{\mu}\hat{R}_L\hat{H}(M_s, M_\theta).\end{aligned}\tag{3.27}$$

Having done this non-dimensionalisation, the governing equations (2.9) remain the same, except for  $\hat{P}$  being replaced by  $P/\epsilon$ , where  $\epsilon = \hat{H}/\hat{R}_L$ . In the indenter region  $\rho$  becomes the ratio of the radii of the indenter and the initial membrane. The constitutive equations (2.17a) become

$$\begin{aligned}T_s &= \frac{1}{\lambda_\theta} \frac{\partial W}{\partial \lambda_s}, \quad M_s = \beta \frac{\lambda_s}{\lambda_\theta} (\lambda_s^2 \kappa_s + \lambda_\theta^2 \kappa_\theta - \kappa_s^R - \kappa_\theta^R) \\ T_\theta &= \frac{1}{\lambda_s} \frac{\partial W}{\partial \lambda_\theta}, \quad M_\theta = \beta \frac{\lambda_\theta}{\lambda_s} (\lambda_s^2 \kappa_s + \lambda_\theta^2 \kappa_\theta - \kappa_s^R - \kappa_\theta^R),\end{aligned}\tag{3.28}$$

where the dimensionless parameter,  $\beta \equiv \frac{\hat{B}}{\hat{\mu}\hat{R}_L^2}$  describes the relative contribution of bending to stretching. If we use the linear elasticity relationship (2.18) we have

$$\beta = \frac{\hat{H}^2}{12\hat{R}_L^2} = \frac{\epsilon^2}{12}.\tag{3.29}$$

### 3.4 Numerical Solution Procedure

To recap, we therefore solve equation (2.9a) in the contact region with the substitutions (3.20) for a given  $\lambda_0$ , to find a solution in which the indenter remains in contact with the shell for a range of  $S$ . This may be done for any  $\beta$ , as the highest derivatives in these equations are not solely multiplied by  $\beta$ .

We then solve the equilibrium equations (2.9) in the free region, adopting a shooting approach on the values of both  $S_c$  and  $\kappa_s(S_c)$ , and integrate through the free region to  $S = L$ .

We then iterate on  $S_c$  and  $\kappa_s(S_c)$  to satisfy the remaining two boundary conditions at  $S = L$ , to find the indentation distance  $\delta$  and force resultant  $F$  for the prescribed  $\lambda_0$ . Varying  $\lambda_0$  then allows us to generate a set of solutions with different indentation distances, allowing us to characterise the entire indentation

process. It should be noted during the integration process, if the initial guesses for  $\kappa_s(S_c)$  and  $S_c$  are too incorrect, the system becomes very stiff or singular when the deformed radius vanishes, especially when the full equations are used and/or  $\beta$  is small (as this is the singular perturbation of the membrane case). The use of continuation of the values from neighbouring values of  $\lambda_0$  therefore greatly helps the convergence of this numerical procedure. All these calculations are undertaken using Mathematica 10 [36], code is available on request.

## 4 Results

### 4.1 Model comparison

Figure 2 shows the comparison between the membrane case as discussed in Pearce et al. [16], and the shell as introduced here, for the indentation of a hemispherical surface by a spherical-tipped indenter ( $\beta = 0.1$ , all other parameters the same). The inclusion of the bending stiffness ensures that the shell requires energy to change the curvature from the reference state. It may be seen that the membrane theory predicts a deformation affecting the entire membrane, with wrinkling (dashed line) occurring across the majority of the membrane, whereas the shell theory predicts a localised deformation. The shell theory also allows for a deformation to be calculated for values of  $\delta$  approaching zero for significantly curved surfaces; as this limit is approached the membrane theory breaks down due to the membrane becoming slack in the indenter region, with both principal stress resultants becoming negative. The approximate theory,  $\nu = 0$ , works well until the reference configuration of the shell becomes extremely curved, at which point neglecting the  $M\kappa$  terms becomes significant. For instance, when the reference configuration is a prolate spheroid with aspect ratio 2.5 (with  $\beta = 0.1$ ,  $\rho = 0.2$ ), the approximate theory predicts a negative force  $F$  for small indentation distances, even though the calculated shape looks fine. This happens as the two terms in (2.10) both tend towards zero, but with the transverse shear being slightly larger. Using the full theory eliminates this counter-intuitive behaviour, but makes the numerical shooting procedure even more sensitive.

We can therefore model the deformation for a range of parameters. We show two further examples, a prolate spheroid (Figure 3) and a sphere being indented from the concave side (Figure 4), showing how the shape of the deformed configuration changes with increasing depth of indentation.

### 4.2 Load-Displacement Curves

Experimentally, the measurable variables during an indentation test are the position of the indenter and the total axial force exerted upon it, in dimensional terms. We are therefore interested in non-dimensional

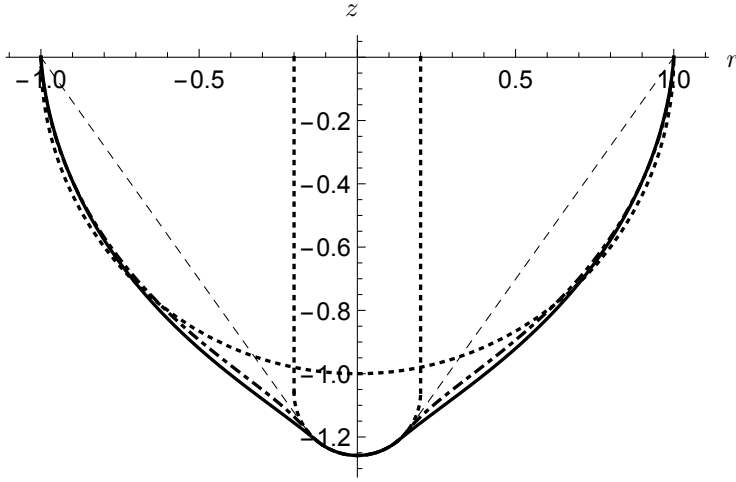


Figure 2: Comparison between the spherical indentation of a hemispherical surface modelled using the membrane model given in Pearce et al. [16] (dashed line), and both the approximate ( $\nu = 0$ , dotdashed line) and full ( $\nu = 1$ , solid line) shell models as described here with  $\beta = 0.1$ . In all cases  $\rho = 0.2$  and the Mooney-Rivlin model is used with  $\alpha = 0.1$ . Dotted lines show the position of the indenter and the undeformed surface.

load-displacement curves generated from solving the equations over a range of  $\lambda_0$ , which we may use to estimate the elastic moduli of the sample by comparison with the experimental curves. In order to generate a non-dimensional load-displacement curve, we need to specify a number of parameters. These are the relative size and shape of the indenter ( $\rho, A, B$ ), the shape of the undeformed shell ( $R, Z$ ), the strain-energy function ( $W$ ) and the bending-stretching ratio  $\beta$ . We shall therefore present here the effect of varying each of these parameters, keeping all the others the same. For each figure the unspecified parameters are a spherical shell and indenter with  $\rho = 0.2, \beta = 0.01$ , a Mooney-Rivlin strain-energy function with  $\alpha = 0.1$  and the full equations  $\nu = 1$ .

As may be intuitively expected, increasing the relative size of the indenter has a strong effect on the total force required to achieve the same deformation, as may be seen in Figure 5, but the shape of the curves are similar.

Increasing the initial curvature of the shell increases the initial steepness of the load-displacement curve, but this increase is not uniform across the depth of indentation for highly curved shells (Figure 6). For these prolate spheroid curves, further indentation does not require as much stretching as they are already highly curved, which is not intuitively obvious.

The choice of strain-energy function only makes a difference to the large strain behaviour, but does have an effect there (Figure 7). The neo-Hookean strain-energy function ( $\alpha = 0$ ) has an unphysical limit at large

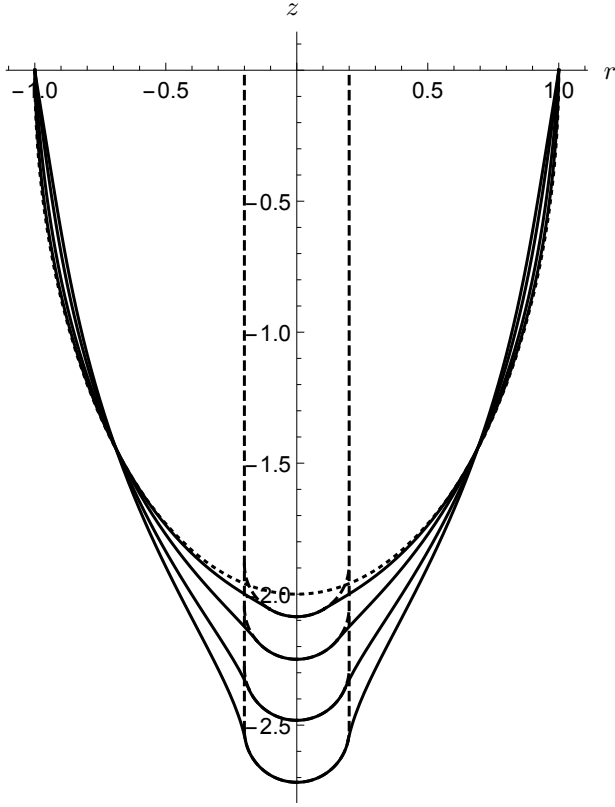


Figure 3: Profile of the deformed configuration for successive depths of indentation of a prolate spheroidal shell,  $\gamma = -2$ , by a spherical indenter with  $\rho = 0.2$  and the Mooney-Rivlin model with  $\alpha = 0.1$ . Dashed lines show the position of the indenter and the undeformed surface.

strain, where increasing displacement does not require any increase in the applied force, as found in the membrane case [16]. Using a strain-hardening strain-energy function such as the Gent model has an even more significant effect, as would be expected (data not shown).

Figure 8 shows that for the approximate theory,  $\nu = 0$ , the bending to stretching ratio  $\beta$ , has only a marginal effect on the required force, even for extremely large values of  $\beta$ , and therefore its main contribution is the regularisation of the problem by enforcing that energy is required to change the initial shape of the membrane. However, when we use the full theory, changing  $\beta$  has a significant effect on the load-indentation curve, as would be expected and is seen in Figure 9. This suggests that the approximate theory is not appropriate for even spherical shells, and the full theory should be used instead.

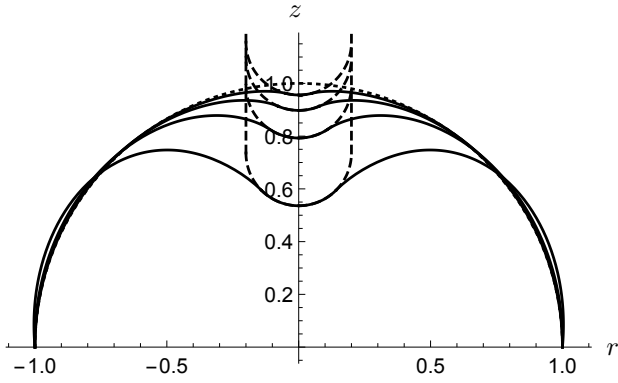


Figure 4: Profile of the deformed configuration for successive depths of indentation of a spherical shell from the concave side,  $\gamma = 1$ , by a spherical indenter with  $\rho = 0.2$  and the Mooney-Rivlin model with  $\alpha = 0.1$ . Dashed lines show the position of the indenter and the undeformed surface.

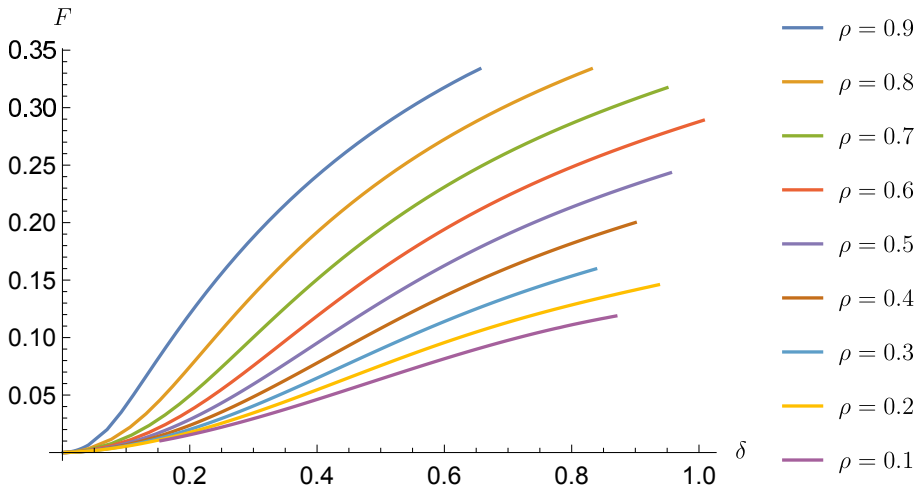


Figure 5: Increasing the size of the indenter,  $\rho$ , requires more force to achieve the same indentation distance.

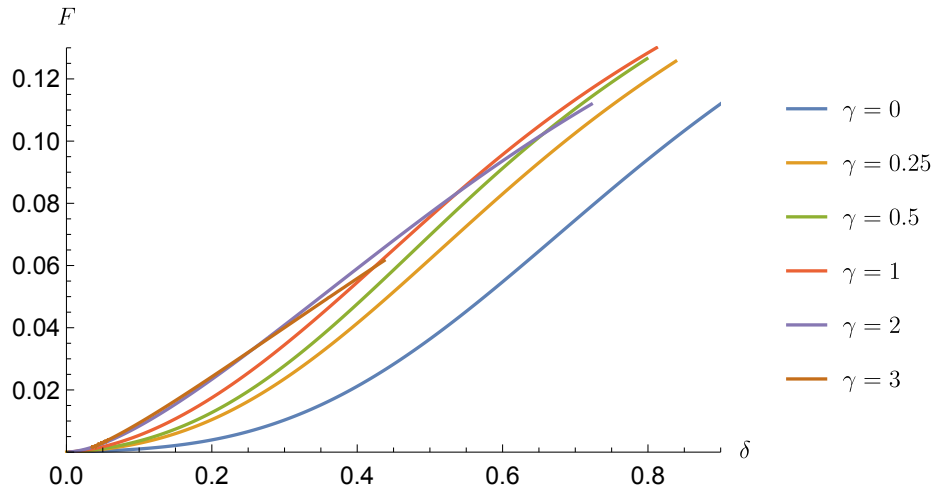


Figure 6: Effect of changing the undeformed shape of the shell,  $R(S) = \sin S, Z(S) = -\gamma \cos S$ .

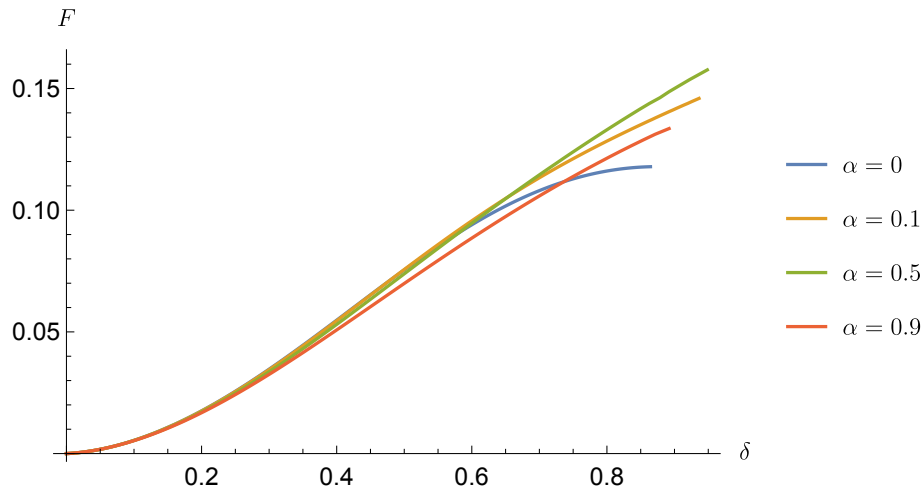


Figure 7: Effect of changing the strain-energy function, by altering the parameter  $\alpha$  in the Mooney-Rivlin constitutive law.



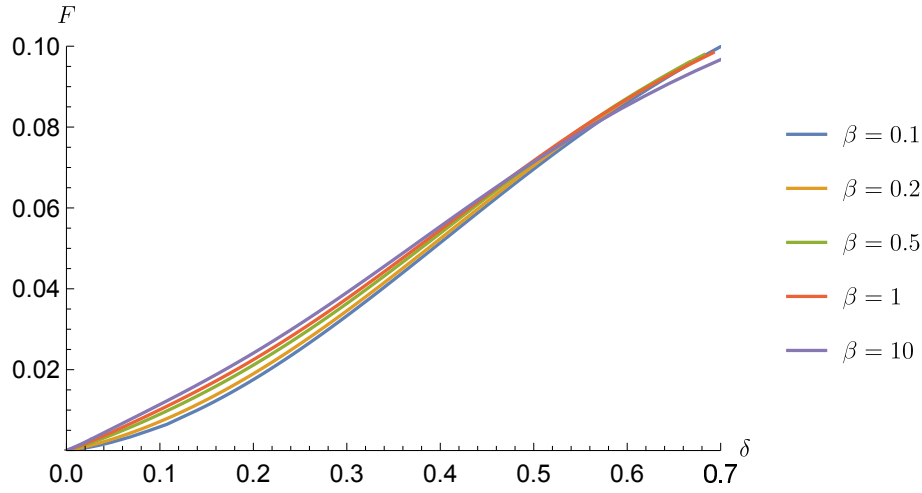


Figure 8: Changing the bending/stretching ratio  $\beta$  with the approximate theory,  $\nu = 0$ , has little impact on the force-displacement curve.

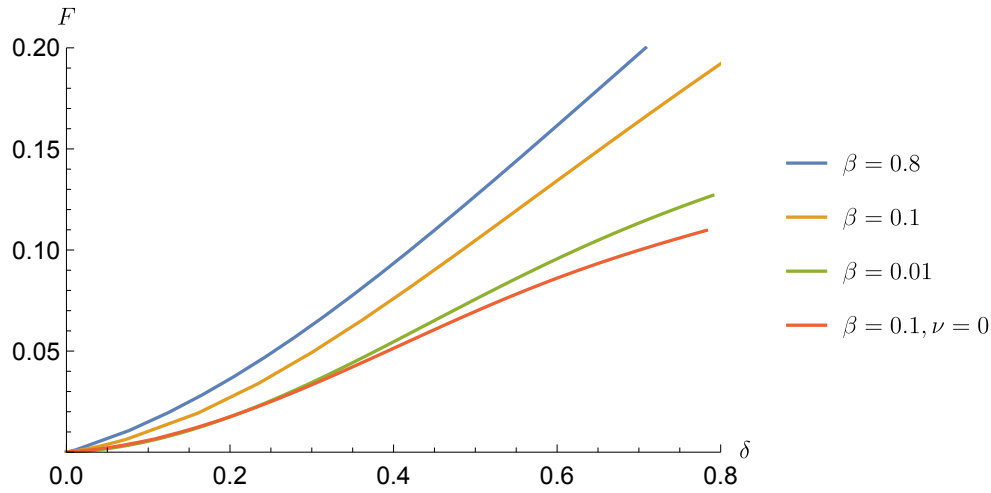


Figure 9: Increasing the bending/stretching ratio  $\beta$  with the full theory,  $\nu = 1$ , increases the force required to indent the shell.

## 5 Conclusions

We have analysed a mathematical model for the finite indentation of a curved elastic shell, which we have developed in order to characterise the elastic properties of a biological sample, although the theory is appropriate for other elastic shells as may be found in engineering or other biological contexts. Within the theory as presented above, the only unknown parameters for the sample are the shear modulus,  $\hat{\mu}$ , the bending modulus,  $\hat{B}$ , and the form of the strain-energy function,  $W$ , including any constants within. It should therefore be possible to fit the moduli first, assuming a suitably precise measuring device, and thus it is only the two moduli that need to be estimated initially, with the strain-energy function only becoming significant if large strains are involved. In this, if (2.18) is used then the two moduli are coupled by the undeformed thickness.

The addition of the bending stiffness into the free region regularises the membrane equations, and allows highly curved surfaces to be considered. In particular, being able to extract an elastic modulus from the experimental force-displacement curves allows the identification of a shape- and size-independent measurement, which may be used to compare between different indented surfaces and is of particular use in a biological context, where the surface shape may vary between samples.

When the shell becomes very highly curved, the approximate theory ( $\nu = 0$ ) breaks down, predicting a negative force for small indentation, and the full theory ( $\nu = 1$ ) must be used. This effect is not dependent on the choice of constitutive law, and entirely comes from the neglecting the contribution of the bending of the shell reference surface. We therefore suggest caution when using the approximate equations for curved shells.

The basis of this model could be extended in a number of directions. The indentation of shells from the concave side could be further considered, particularly in combination with an internal pressure  $P$ ; this would change the pre-indentation shape of the shell (and hence change the boundary condition at  $\lambda_\theta(L)$ ) but the governing equations are unchanged. Combined these two extensions allow for the modelling of the indentation of shells with an internal pressure, such as inflated balls, balloons or biological tissues. Other extensions to non-uniform undeformed thickness, different initial configurations (such as complete shells) or a bending energy that depends on further invariants of  $\Delta$  are also possible.

As mentioned in the introduction, we are interested in using this model to estimate the elastic properties of seed endosperms; this work will be presented elsewhere.

## Acknowledgements

This work was initially funded by an ERANET-PG grant for the vSEED project (BBSRC grant BBG02488X1). SPP thanks the Leverhulme Trust for the award of an Early Career Fellowship. JRK additionally acknowledges the support of the Royal Society and the Wolfson Foundation. SPP additionally thanks to many people with whom he has discussed the negative forces.

## Appendix

In this Appendix we briefly give the equations to show the two-dimensional theory of Steigmann and Ogden [24] gives the governing equations (2.9). The tangent vectors are given by,

$$\mathbf{g}_1 = \frac{\partial \mathbf{x}}{\partial \theta} = r \mathbf{e}_\theta, \quad \mathbf{g}_2 = \frac{\partial \mathbf{x}}{\partial S} = r' \mathbf{e}_r + z' \mathbf{e}_z = \psi \mathbf{e}_s, \quad (\text{A.1})$$

where here and elsewhere we identify the first coordinate as  $\theta$  and the second coordinate as  $S$ . The non-zero metric components are then given by  $g_{11} = r^2, g_{22} = \psi^2$ . The 2-dimensional deformation gradient,  $\mathbf{F}$ , becomes

$$\mathbf{F} = \frac{r}{R} \mathbf{e}_\theta \otimes \mathbf{E}_\theta + \frac{\psi}{\Psi} \mathbf{e}_s \otimes \mathbf{E}_s = \lambda_\theta \mathbf{e}_\theta \otimes \mathbf{E}_\theta + \lambda_s \mathbf{e}_s \otimes \mathbf{E}_s. \quad (\text{A.2})$$

The right Cauchy-Green tensor,  $\mathbf{C}$  is given by

$$\mathbf{C} = \mathbf{F}^T \mathbf{F} = \frac{r^2}{R^2} \mathbf{E}_\theta \otimes \mathbf{E}_\theta + \frac{\psi^2}{\Psi^2} \mathbf{E}_s \otimes \mathbf{E}_s, \quad (\text{A.3})$$

showing the squares of the two principal stretches within the shell. The reference curvature tensor  $\mathbf{B}$  is

$$\mathbf{B} = B_{\alpha\beta} \mathbf{G}^\alpha \otimes \mathbf{G}^\beta = \kappa_\theta^R \mathbf{E}_\theta \otimes \mathbf{E}_\theta + \kappa_s^R \mathbf{E}_s \otimes \mathbf{E}_s. \quad (\text{A.4})$$

The relative curvature tensor,  $\boldsymbol{\kappa}$ , is

$$\boldsymbol{\kappa} = \kappa_{\alpha\beta} \mathbf{G}^\alpha \otimes \mathbf{G}^\beta = \frac{\kappa_{11}}{R^2} \mathbf{E}_\theta \otimes \mathbf{E}_\theta + \frac{\kappa_{22}}{\Psi^2} \mathbf{E}_s \otimes \mathbf{E}_s, \quad (\text{A.5})$$

where the covariant components  $\kappa_{\alpha\beta}$  are defined by (and transformed to the mixed components using the metric tensor)

$$\kappa_{11} = \frac{r z'}{\psi} = r^2 \kappa_\theta, \quad \kappa_{22} = \frac{z'' r' - r'' z'}{\psi} = \psi^2 \kappa_s. \quad (\text{A.6})$$

The relative curvature strain tensor  $\boldsymbol{\Delta}$ , of which the invariants  $I_3$  and  $I_4$  are defined is therefore given by

$$\boldsymbol{\Delta} = \boldsymbol{\kappa} - \mathbf{B} = \left( \frac{\kappa_{11}}{R^2} - \kappa_\theta^R \right) \mathbf{E}_\theta \otimes \mathbf{E}_\theta + \left( \frac{\kappa_{22}}{\Psi^2} - \kappa_s^R \right) \mathbf{E}_s \otimes \mathbf{E}_s. \quad (\text{A.7})$$

The right hand side of the governing equations (4.21c) in Steigmann and Ogden [24] then becomes

$$\begin{aligned}
(G^{1/2}\mathbf{P}^\alpha)_{,\alpha} = & \left( \left( G^{1/2} J \psi [\sigma^{22} + \kappa_s m^{22}] \right)' - \left( G^{1/2} J [\sigma^{11} + \kappa_\theta m^{11}] \frac{rr'}{\psi} \right) \right. \\
& + \kappa_s \left\{ (G^{1/2} J m^{22} \psi)' - G^{1/2} J m^{11} \frac{rr'}{\psi} \right\} \Bigg) \mathbf{e}_s \\
& \left( -\kappa_s (G^{1/2} J [\sigma^{22} + \kappa_s m^{22}] \psi^2) - \kappa_\theta \left( G^{1/2} J [\sigma^{11} + \kappa_\theta m^{11}] r^2 \right) \right. \\
& \left. \left. + \left[ \frac{1}{\psi} \left\{ (G^{1/2} J m^{22} \psi)' - (G^{1/2} J m^{11} \frac{rr'}{\psi}) \right\} \right]' \right) \right) \mathbf{n} \quad (\text{A.8})
\end{aligned}$$

where we have used the Frenet-Serret relations (2.7) and the definitions  $g^{1/2} = r\psi h$ ,  $G^{1/2} = R\Psi H$ ,  $J = g^{1/2}G^{-1/2}$  from Steigmann and Ogden [24]. To reduce to (2.9), we require the connections  $\hat{T}_i = \hat{h}\sigma_i^i$ ,  $\hat{m}_i = \hat{h}M_i^i$ , as well as the use of the metric tensor to transform to mixed components using  $\sigma_i^i = g_{ii}\sigma^{ii}$ ,  $M_i^i = g_{ii}M^{ii}$ .

## References

- [1] J. D. Humphrey. Review: Computer Methods in Membrane Biomechanics. *Computer methods in biomechanics and biomedical engineering*, 1(3):171, 1998.
- [2] Narain Mulchand Bhatia and W Nachbar. Finite indentation of an elastic membrane by a spherical indenter. *International Journal of Non-Linear Mechanics*, 3(3):307–324, 1968.
- [3] W. H. Yang and K. H. Hsu. Indentation of a circular membrane. *Journal of Applied Mechanics*, 38: 227–229, 1971.
- [4] T. Chudoba, N. Schwarzer, and F. Richter. Determination of elastic properties of thin films by indentation measurements with a spherical indenter. *Surface and Coatings Technology*, 127(1):9–17, 2000.
- [5] M. R. Begley and T. J. Mackin. Spherical indentation of freestanding circular thin films in the membrane regime. *Journal of the Mechanics and Physics of Solids*, 52(9):2005–2023, 2004.
- [6] C. T. Nguyen and T. Vu-Khanh. Mechanics and mechanisms of puncture of elastomer membranes. *Journal of Materials Science*, 39(24):7361–7364, 2004.
- [7] U. Komaragiri, M. R. Begley, and J. G. Simmonds. The mechanical response of freestanding circular elastic films under point and pressure loads. *Journal of Applied Mechanics*, 72:203, 2005.
- [8] D. J. Steigmann. Puncturing a thin elastic sheet. *International Journal of Non-linear Mechanics*, 40(2-3): 255–270, 2005.
- [9] B. Nadler and D. J. Steigmann. Modeling the indentation, penetration and cavitation of elastic membranes. *Journal of the Mechanics and Physics of Solids*, 54(10):2005–2029, 2006.
- [10] Amir HA Deris and Ben Nadler. Modeling the indentation and puncturing of inflated elastic membranes by rigid indenters. *International Journal of Non-Linear Mechanics*, 69:29–36, 2015.
- [11] D. Vella, A. Ajdari, A. Vaziri, and A. Boudaoud. The indentation of pressurized elastic shells: from polymeric capsules to yeast cells. *Journal of the Royal Society Interface*, 9:448–455, 2012.
- [12] D. Vella, A. Ajdari, A. Vaziri, and A. Boudaoud. Indentation of ellipsoidal and cylindrical elastic shells. *Physical Review Letters*, 109, 2012.
- [13] Julien Chopin, Dominic Vella, and Arezki Boudaoud. The liquid blister test. *Proceedings of the Royal Society of London A: Mathematical, Physical and Engineering Sciences*, 464(2099):2887–2906, 2008.
- [14] M.H. Zhao, W.L. Zheng, C.Y. Fan, and E. Pan. Nonlinear elastic mechanics of the ball-loaded blister test. *International Journal of Engineering Science*, 49(9):839–855, 2011.

- [15] K. Wan and K. Liao. Measuring mechanical properties of thin flexible films by a shaft-loaded blister test. *Thin Solid Films*, 352(1):167–172, 1999.
- [16] S. P. Pearce, J. R. King, and M. J. Holdsworth. Axisymmetric indentation of curved elastic membranes by a convex rigid indenter. *International Journal of Non-Linear Mechanics*, 46:1126–1138, 2011.
- [17] A. C. Pipkin. The relaxed energy density for isotropic elastic membranes. *IMA journal of applied mathematics*, 36(1):85, 1986.
- [18] H. Andra, M. K. Warby, and J. R. Whiteman. Contact problems of hyperelastic membranes: existence theory. *Mathematical methods in the applied sciences*, 23(10):865–895, 2000.
- [19] K. Muller, S. Tintelnott, and G. Leubner-Metzger. Endosperm-limited Brassicaceae seed germination: abscisic acid inhibits embryo-induced endosperm weakening of *Lepidium sativum* (cress) and endosperm rupture of cress and *Arabidopsis thaliana*. *Plant and cell physiology*, 47(7):864–877, 2006.
- [20] S. Timoshenko and S. Woinowsky-Krieger. *Theory of Plates and Shells*. McGraw-Hill, second edition, 1959.
- [21] S. P. Preston, O. E. Jensen, and G. Richardson. Buckling of an axisymmetric vesicle under compression: the effects of resistance to shear. *Quarterly Journal of Mechanics and Applied Mathematics*, 61(1):1–24, 2008.
- [22] D. C. Pamplona, J. A. Greenwood, E. Reader, and C. R. Calladine. The buckling of spherical liposomes. *Journal of biomechanical engineering*, 127:1062, 2005.
- [23] P. R. Zarda, S. Chien, and R. Skalak. Elastic deformations of red blood cells. *Journal of Biomechanics*, 10(4):211–221, 1977.
- [24] D. J. Steigmann and R. W. Ogden. Elastic surface-substrate interactions. *Proceedings: Mathematical, Physical and Engineering Sciences*, 455(1982):437–474, 1999.
- [25] JR Sanders and J Lyell. Nonlinear theories for thin shells. *Quarterly of Applied Mathematics*, pages 21–36, 1963.
- [26] Anthony Kwok-Cheung Yeung. Mechanics of inter-monolayer coupling in fluid surfactant bilayers, 1994.
- [27] Augustus Edward Hough Love. *A treatise on the mathematical theory of elasticity*. Cambridge University Press, fourth edition edition, 1927.
- [28] W. Pietraszkiewicz. Geometrically nonlinear theories of thin elastic shells. *Advances in Mechanics*, 12(1):51–130, 1989.

- [29] W. Pietraszkiewicz. Explicit lagrangian incremental and buckling equations for the non-linear theory of thin shells. *International Journal of Non-Linear Mechanics*, 28(2):209–220, 1993.
- [30] S Opoka and W Pietraszkiewicz. On modified displacement version of the non-linear theory of thin shells. *International Journal of Solids and Structures*, 46(17):3103–3110, 2009.
- [31] M. G. Blyth and C. Pozrikidis. Solution space of axisymmetric capsules enclosed by elastic membranes. *European Journal of Mechanics/A Solids*, 23(5):877–892, 2004.
- [32] E Evans and A Yeung. Hidden dynamics in rapid changes of bilayer shape. *Chemistry and Physics of Lipids*, 73(1-2):39–56, 1994.
- [33] R. W. Ogden. *Non-linear elastic deformations*. Dover Publications, 1997.
- [34] PM Naghdi and PY Tang. Large deformation possible in every isotropic elastic membrane. *Philosophical Transactions for the Royal Society of London. Series A, Mathematical and Physical Sciences*, 287(1341):145–187, 1977.
- [35] D. M. Haughton. Elastic membranes. In Y. B. Fu and R. W. Ogden, editors, *Nonlinear Elasticity: Theory and Applications*. Cambridge University Press, 2001.
- [36] Wolfram Research Inc. *Mathematica 10.0*. Champaign, Illinios, 2014.